Journal of Cellular Biochemistry 102:1180–1189 (2007)

Functional Three-Dimensional HepG2 Aggregate Cultures Generated From an Ultrasound Trap: Comparison With HepG2 Spheroids

Jian Liu,[1]* Larisa A. Kuznetsova,[2] Gareth O. Edwards,[2] Jinsheng Xu,[1] Mingwen Ma,[1] Wendy M. Purcell,[3] Simon K. Jackson,[1] and W. Terence Coakley[2]

[1]Centre for Research in Biomedicine, Faculty of Applied Sciences, University of the West of England, Coldharbour Lane, Bristol BS16 1QY, UK
[2]School of Biosciences, Cardiff University, Cardiff CF10 3TL, UK
[3]Health and Human Sciences Research Institute, University of Hertfordshire, Hatfield AL10 9AB, UK

Abstract Three-dimensional culture systems are an ideal in vitro model being capable of sustaining cell functionalities in a manner that resembles the in vivo conditions. In the present study, we developed an ultrasound trap-based technique to rapidly produce HepG2 hepatocarcinoma cell aggregates within 30 min. Enhanced junctional F-actin was observed at the points of cell–cell contact throughout the aggregates. HepG2 aggregates prepared by the ultrasound trap can be maintained in culture on a P-HEMA-coated surface for up to 3 weeks. The cells in these aggregates proliferated during the initial 3 days and cell number was consistent during the following maintenance period. Albumin secretion from these HepG2 aggregates recovered after 3 days of aggregate formation and remained relatively stable for the following 12 days. Cytochrome P450-1A1 activity was significantly enhanced after 6 days with maximal enzyme activity observed between 9 and 18 days. In addition, comparison experiments demonstrated that HepG2 aggregates generated by the ultrasound trap had comparable functional characterizations with HepG2 spheroids formed by a traditional gyrotatory-mediated method. Our results suggest that HepG2 aggregate cultures prepared through the ultrasound trap-based technique may provide a novel approach to produce in vitro models for hepatocyte functional studies. J. Cell. Biochem. 102: 1180–1189, 2007.

Key words: 3D culture; USWT; HepG2; F-actin; proliferation; albumin; P450-1A1

Although three-dimensional (3D) aggregate cultures have been used in laboratories for more than 60 years [Holtfreter, 1944], it was only 30 years ago that the 3D cell culture models were widely explored by the scientific community [Sutherland et al., 1971; Mueller-Klieser, 1997; Santini and Rainaldi, 1999]. Compared to conventional monolayer cultures, artificial constructs of robust 3D multicellular masses (3DMMs) show different or even opposite cell behavior including long culture period, regulated gene production, stable drug metabolism functions, quiescent cell populations resistant to chemotherapeutic drugs and more closely resemble the in vivo situation [Khalil et al., 2001; Ma et al., 2003; Xu et al., 2003a; Mellor et al., 2005]. Although the molecular mechanisms of 3D multicellular cultures still need to be understood in detail, these in vivo like in vitro models offer an efficient tool in a variety of experimental and clinical studies [Mueller-Klieser, 1997; Kunz-Schughart et al., 2004].

Over the years, a number of techniques have been devised and developed to generate multicellular cultures in vitro. For example, spontaneous aggregation of cells occurs on non-adherent substrates such as agarose and the commercial Primaria dish [Yuhas et al., 1977; Lin et al., 2006]. Encapsulation of cells in biochemical scaffolds like collagen, alginate beads or galactosylated nanofibers has successfully produced different types of aggregate cultures [Bell et al., 1979; Papas et al., 1993; Chua et al., 2005]. In addition, gyrotatory-

Grant sponsor: Biotechnology and Biological Sciences Research Council; Grant number: BB/C515220/1.

*Correspondence to: Dr. Jian Liu, University of the West of England, Centre for Research in Biomedicine, Bristol BS16 1QY. E-mail: jian.liu@uwe.ac.uk

Received 14 December 2006; Accepted 28 February 2007
DOI 10.1002/jcb.21345

mediated methods have been used to obtain 3D spheroid cultures [Sutherland et al., 1971; Sakai et al., 1996; Ma et al., 2003; Xu et al., 2003a].

An ultrasound standing wave trap (USWT)-based technique was recently developed to synchronously and rapidly generate multicellular aggregates in suspension away from the influence of a solid substrate [Bazou et al., 2005, 2006]. The technique employed for making multicellular aggregates utilizes the phenomenon of particle aggregation in USWT (Fig. 1A–C). Standing waves are produced from the superimposition of two waves of the same frequency travelling in opposite directions. These two waves are either generated from two different sources, or the initial wave is reflected from a solid boundary. Such waves are characterized by lack of vibration at certain points (acoustic pressure nodes), between which areas of maximum vibration occur periodically (acoustic pressure anti-nodes). Suspended cells in USWT are affected by the direct acoustic radiation force (DRF) [Gor'kov, 1962]. The stronger, axial component drives particles towards the pressure node planes, whereas the lateral components, which are about two orders of magnitude smaller, act within the planes and concentrate particles/cells laterally into clumps.

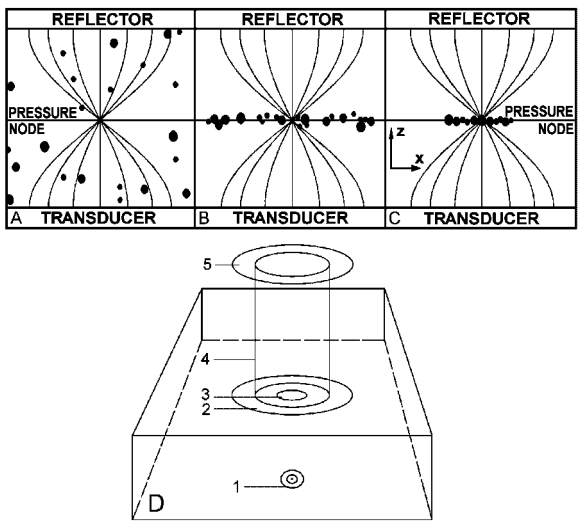

Fig. 1. Schematics of the ultrasound standing wave trap (USWT). **A–C**: Direct acoustic radiation force (DRF) affects suspended particles in a resonator with λ/2 water path length depth. A: Distribution of particles before ultrasound application. B: Axial DRF effect. C: Lateral DRF effect. Reproduced with permission from Kuznetsova and Coakley [2004]. **D**: Design of the resonator. 1, electrical connection; 2, piezoelectric transducer; 3, transducer's etched area; 4, plastic tube containing sample volume; 5, 1 mm-thick glass reflector. (x: lateral direction and z: direction of sound propagation.)

Previous reports have demonstrated that an ultrasound trap can generate 2D cell aggregates in suspensions from neural cells and chondrocytes, leading to the development of the cytoskeleton and adhesion molecules within 1 h [Bazou et al., 2005, 2006]. These studies showed the rapid molecular development at cell–cell contacts of 2D aggregates in very early stage (up to 60 min) after formation in the USWT. However, the application of the newly developed ultrasound trap-based technique for the generation of 3D cell cultures, long-term maintenance in culture and cell functional characteristics of such aggregates have not yet been investigated.

In the present study, we produced 3D HepG2 hepatocarcinoma cell aggregates using a developed USWT (Fig. 1D) and maintained the aggregates in culture for up to 3 weeks. The filamentous-actin (F-actin) distribution, cell proliferation, and two parameters for liver-specific functions namely albumin secretion and cytochrome P450-1A1 activity were examined in HepG2 USWT aggregates. All characterizations of HepG2 USWT aggregates assessed in this study were compared with HepG2 spheroids generated by the traditional gyrotatory-mediated method [Xu et al., 2003a; Ma et al., 2003]. To the best of our knowledge, this is the first report investigating the maintenance and characteristics of 3D cell culture produced through an ultrasound trap-based technique.

MATERIALS AND METHODS

Cell Culture

The human Caucasian Hepatocellular cancer cell line HepG2 (European Collection of Cell Cultures, Salisbury, UK) was cultured in DMEM (Sigma–Aldrich, Gillingham, UK) supplemented with 10% fetal bovine serum, 1% non-essential amino acids, 200 nM L-glutamine, and 100 U/ml penicillin and 100 μg/ml streptomycin (Invitrogen, Paisley, UK) with subculturing performed with 0.05% trypsin/0.02% EDTA (Sigma–Aldrich) at a split ratio of 1:5. Subcultured cells were allowed to recover for at least 2 days before performing experiments to form aggregates using either ultrasound equipment or gyrotatory shaking.

Ultrasonic Technique and Acoustic Chamber

The design of the cylindrical multi-wavelength resonator with a disk piezoelectric transducer is shown in Figure 1D. The thickness of the 25 mm diameter transducer was 1 mm so that the transducer's nominal thickness resonance frequency was 2 MHz. The plastic cylindrical tube of 26 mm height and 13 mm inner diameter was glued to the transducer and contained 3.5 ml of sample. The transducer's electrodes were etched to produce an active radiation area of 6 mm in diameter. A 1-mm thick, 25-mm diameter quartz glass (Heraeus Quarzglas, Surrey, UK) was used as a reflector. A Hewlett Packard 33120A function synthesizer provided a sine wave input to an ENI 2100L amplifier, and the voltage across the transducer was monitored on an oscilloscope. The software STAND controlled the ultrasound equipment and allowed preliminary determination of the resonance conditions by scanning the voltage–frequency spectra from a voltmeter [Hawkes and Coakley, 1996]. The frequency of 2.24 MHz was maintained during the experiments.

Ultrasound Cell Aggregates Formation and Maintenance

HepG2 single cell suspensions for ultrasound aggregation experiments were obtained by incubation of monolayers with Accutase (Sigma–Aldrich) that leaves most of the cell surface molecules intact [Nitori et al., 2005]. The chamber and the cover glass were sterilized with 70% ethanol. The chamber was filled with HepG2 cells suspended in cell culture media (6.5×10^5 cell/ml) and sealed with the cover glass in sterile conditions. It was then immediately connected to the ultrasound equipment and sonication was initiated. The cell aggregates were formed within 1 min at 60 V across the transducer, after which the voltage was reduced and maintained at 20 V to prevent the system from overheating. The temperature measured on the resonator's surface with a portable infrared thermometer (Raynger®ST™, Santa Cruz, CA, USA) did not exceed 32°C during the time of experiments. Cell movement was monitored with a standard PAL CCD JVC video camera (Victor Company, Tokyo, Japan), which was connected via a 0.5 microscope adaptor to a TV. The images were also recorded onto standard videotape. The recorded video sequences were transferred to a PC video card in digital format with hardware MJPEG data compression (Pinnacle Miro Video DC30+). After 30 min of application the ultrasound was turned off and the disc-like cell aggregates were carefully removed from the chamber under sterile conditions. The cell concentration was adjusted to 2×10^5 cells/ml with fresh culture medium and 0.5 ml of the aggregate suspension was seeded and maintained in each well of 24-well tissue culture plates precoated with 0.5 ml of 2.5% poly (2-hydroxyethyl methacrylate) (P-HEMA, Sigma–Aldrich) dissolved in 95% ethanol. The culture media were replaced every 3 days with fresh media.

Spheroid Culture

HepG2 spheroids were generated by a gyrotatory-mediated method according to a previous study [Ma et al., 2003]. Briefly, HepG2 monolayer cultures were detached using 0.05% trypsin/0.02% EDTA solution (Sigma–Aldrich) and 3 ml of single cell suspension (1×10^6 cell/ml) was added to each well of six-well plates. The plates were placed on a gyrotatory shaker (New Brunswick, St. Albans, UK) at 83 rpm for the first 24 h, and rotated at 77 rpm thereafter. The cell culture media were replaced every 3 days with fresh media.

Fluorescence Staining of F-Actin

HepG2 aggregates generated in USWT for 30 min were fixed in 90% ethanol for 20 min on Histobond slides (Raymond A. Lamb Ltd., Eastbourne, UK). Samples were washed in PBS, permeabilised for 30 min with 0.1% Triton X-100 (Sigma–Aldrich) and blocked for 30 min with 1% BSA (Sigma–Aldrich). F-actin was stained for 20 min with 10 u/ml Phalloidin-Alexa 488 conjugate (Invitrogen) and mounted in VectaShield containing DAPI (Vector Laboratories, Peterborough, UK). The stained USWT aggregates were examined with an Olympus BX41 microscope and images for epifluorescence of F-actin were captured using an Olympus DP-SOFT software (Version 3.1).

To determine the maintenance of junctional F-actin during aggregate maintenance, both HepG2 aggregates prepared by the USWT and HepG2 spheroids generated by the gyrotatory-mediated method were stained at different time points during culture with Phalloidin-Alexa 488 conjugate as described above with the exception

of cell permeabilisation. Confocal micrographs of F-actin were captured by a Nikon PCM2000 Confocal Laser Scanning Microscope (CLSM) using the COORD EZ2000 software.

Cell Proliferation Assay

At different time points during the aggregate culture, cell proliferation was assessed using a colorimetric assay based on the cleavage of a tetrazolium salt by cellular mitochondrial dehydrogenase activity (WST-1, Roche, Mannheim, Germany). One-unit volume of the WST-1 reagent was added to 10-unit volume of cell culture suspensions, incubated for 60 min at 37°C. The absorbance was read at 450 nm using a Multiscan RC microplate reader (Labsystems, Basingstoke, UK). The proliferation index was calculated as the percentage of cell number on the sampling day versus that on the day of aggregate formation.

Immunoassay for Albumin Secretion

Aggregate culture medium was replaced with serum-free medium at indicated time points and aggregates were incubated in the serum-free medium for 6 h. Culture supernatants were then harvested and stored at −80°C until analysis for albumin concentrations by a sandwich enzyme-linked immunosorbent assay (ELISA) kit according to the manufacturer's instructions (Bethyl Laboratories, Montgomery, TX, USA). The albumin concentrations were calibrated against total cellular protein as measured using a Protein Assay Kit (Bio-Rad Laboratories, Hemel Hempstead, UK).

P450-1A1 Activity

Cytochrome P450-1A1 enzyme activity of HepG2 aggregates was measured using the ethoxyresorufin-*O*-deethylase (EROD) assay [Klotz et al., 1984; Peters et al., 2004]. The EROD converts ethoxyresorufin to resorufin that reflects the P450-1A1 activity. At different time points, cell culture medium was replaced with fresh medium containing the specific P450-1A1 inducer β-naphthoflavone (final concentration 50 μM, Sigma–Aldrich) and aggregates were incubated for 24 h. The induction medium was then replaced with fresh medium containing 20 μM ethoxyresorufin (Sigma–Aldrich), along with 200 μM probenecid (Sigma–Aldrich) to prevent subsequent metabolism of resorufin. After a further 30 min of incubation, the cell culture supernatants were collected and resorufin concentrations were determined at em/ex 560/586 nm using a LS-50B fluorescence spectrometer (Perkin-Elmer, Beaconsfield, UK). The resorufin concentrations were calibrated by total cell protein.

Statistical Analysis

Data were presented as mean ± SD. Results were analyzed using the two-tailed Student's *t*-test and differences were considered significant at $P < 0.05$.

RESULTS

Formation of Cell Aggregates in USWT

Within 80 ms of ultrasound initiation, the evenly distributed cells in suspension came under the influence of the axial direct radiation force and moved to the pressure node planes forming multiple horizontal layers (Fig. 2A). Since the transducer's electrodes were etched, the lateral components of the radiation force concentrated the cells in aggregates at λ/2 intervals at the central axis of the chamber (Fig. 2B). This pattern was maintained during the entire period (30 min) of sonication.

F-Actin Cytoskeleton Reorganization in USWT Aggregates

Epifluorescence microscopy showed that F-actin was notably detected at points of cell–cell contact in a pattern of thick and continuous band (junctional F-actin, marked with arrowheads) throughout the HepG2 aggregate prepared by 30 min sonication in the USWT (Fig. 3A). In the unsonicated single cell, F-actin was distributed throughout the cytoplasm and there was less prominent labeling around the cell periphery (Fig. 3A, inset).

Stable F-Actin Distribution During Aggregate Maintenance

After formation of 3-D HepG2 aggregates in the USWT, the aggregates were transferred to P-HEMA precoated plates for maintenance. The shape of aggregates was maintained in culture and the aggregates retained intact for 18 days (Fig. 3B–D). Fluorescence staining and confocal microscopy demonstrated that F-actin distribution including the junctional F-actin throughout the aggregates remained consistent during maintenance with no observable changes between 1 and 18 days (Fig. 3C and D).

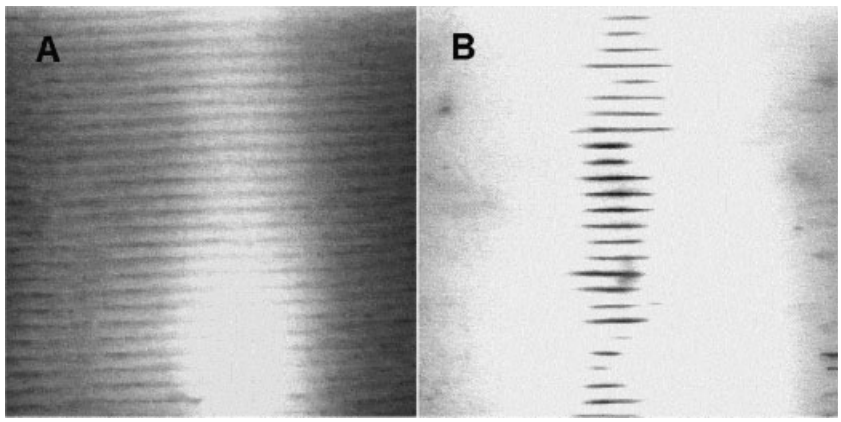

Fig. 2. HepG2 cell aggregates generated in USWT. **A**: Layers of cells in pressure node planes at λ/2 intervals. **B**: Cell aggregates in the axial region.

The HepG2 aggregates generated and subsequently maintained by the gyrotatory technique exhibited morphological changes during culture. Single cells in suspension started to fuse after 2 h of plating (Fig. 3E). After 24 h, small and irregular aggregates appeared and possessed significant junctional F-actin (Fig. 3F). Spherical aggregates at approximately 60 μm diameter formed after 3 days and gradually increased in size with increasing culture time due to the fusion of smaller aggregates (Fig. 3G–I). F-actin fluorescence in the center of spheroids of 9 or more days old could not be detected as they had become too thick (about 200 μm in diameter), resulting in dark areas observed in the centre of the stained spheroids.

Cell Proliferation

To investigate the HepG2 cell proliferation in 3D aggregates generated by the gyrotatory method or USWT, proliferation assays were applied during aggregate maintenance. In gyrotatory spheroids, no significant cell proliferation was observed and the cell number remained stable during the culture period (Fig. 4A). In contrast, cells in USWT aggregates (Fig. 4B) demonstrated significantly increased cell number during the initial 3 days after aggregate formation ($P = 0.034$ for 1 day versus 0 day, $P = 0.002$ for 3 day versus 1 day), followed by reaching a plateau between 3 and 21 days ($P > 0.05$).

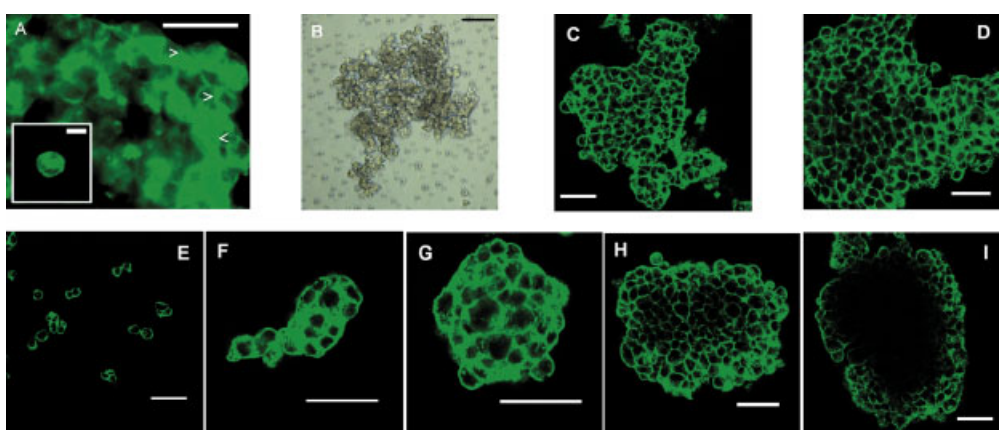

Fig. 3. Morphology and F-actin staining of HepG2 aggregates. **A**: Epifluorescence micrograph of F-actin stained with Phalloidin-Alexa 488 in 3D aggregates generated in the USWT. Examples of junctional F-actin are marked with arrowheads (bar 25 μm). Inset shows an unsonicated single cell (bar 10 μm). **B**: Light microscope observation of the USWT aggregate maintained on a P-HEMA-coated surface after 1 day of aggregate formation in USWT. **C** and **D**: Confocal micrograph of F-actin staining in USWT aggregates after 1 day (C) and 18 days (D). **E–I**: Confocal micrograph of F-actin staining in gyrotatory-produced aggregates after 2 h (E), 1 day (F), 3 days (G), 9 days (H) and 18 days (I) (B–I, bar 50 μm). [Color figure can be viewed in the online issue, which is available at www.interscience.wiley.com.]

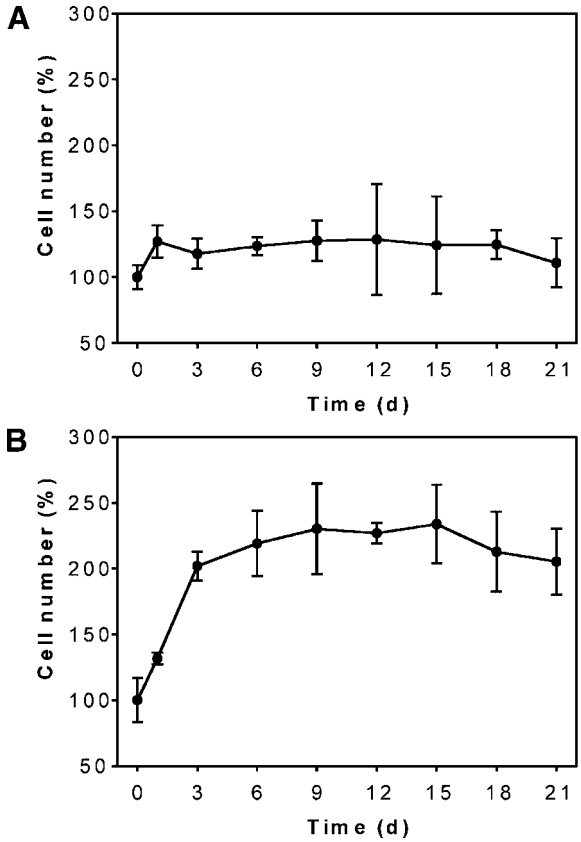

Fig. 4. Cell proliferation studies of HepG2 aggregates. Cell numbers in gyrotatory spheroids (**A**) and USWT aggregates (**B**) were measured at the indicated time points using a cell proliferation reagent WST-1. Three independent experiments with triplicates were performed.

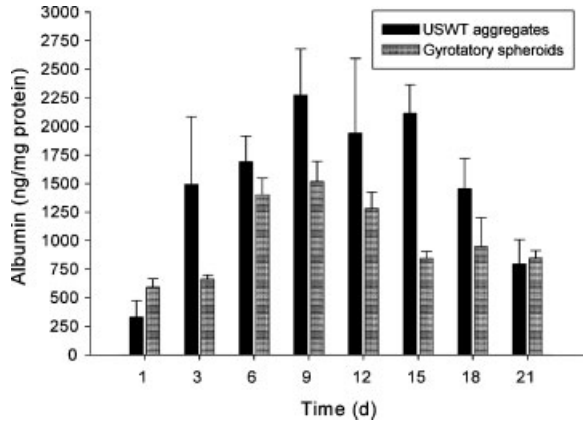

Fig. 5. Comparison of kinetics of albumin release from HepG2 USWT aggregates and gyrotatory spheroids. At indicated time points, the cells were treated with serum-free medium for 6 h and culture supernatants were then collected. The concentrations for human albumin in culture supernatants were determined using ELISA and normalized by cell protein amount. Data are obtained from three separate experiments with two to three replicate samples.

Recovered Albumin Secretion

The time-dependent albumin secretion by HepG2 USWT aggregates during maintenance is shown in Figure 5. Albumin secretion levels sharply increased after three days of aggregate formation in USWT as compared with day 1 ($P = 0.029$), followed by a relatively stable phase between 3 and 15 days ($P > 0.05$). After 18 days, the albumin release started to decrease ($P = 0.035$ for 18 days versus 15 days, $P = 0.028$ for 21 days versus 18 days). In comparison, spheroid aggregates showed delayed recovery of albumin secretion (Fig. 5). The albumin secretion level after 1 day was slightly higher than USWT aggregates ($P = 0.1$). Increased albumin secretion was observed between 6 and 12 days ($P < 0.01$ versus 1 day) followed by decreased secretion during 15–21 days. In addition, the overall albumin secretion of gyrotatory spheroids between 3 and 18 days of maintenance in culture showed lower levels than USWT aggregates, although significant difference was only found after 15 days ($P = 0.007$).

Recovered P450-1A1 Activity

The production amount of resorufin at different time points during aggregate culture represents the kinetics of cell P450-1A1 activity. As shown in Figure 6, the enzyme activity of USWT aggregates was slightly enhanced at day 3 compared to day 1 ($P = 0.11$), followed by a steady increase between 3 and 9 days ($P = 0.036$ for 6 days versus 3 days, $P = 0.030$ for 9 days versus 6 days). A stable phase for P450-1A1 activity was demonstrated between 9 and 18 days. In HepG2 spheroids, the enzyme activity started to increase after 6 days ($P = 0.031$ for 6 days versus 3 days, $P = 0.015$ for 9 days versus 6 days) and remained stable until 18 days. Similar to albumin secretion, higher P450-1A1 activity levels of HepG2 USWT aggregates between 3 and 21 days were observed compared to gyrotatory-prepared spheroids.

DISCUSSION

In comparison with monolayer hepatocytes, the generation of 3D hepatocyte cultures in vitro produces efficient models that are more similar to the in vivo situation in term of cell morphology, functionality and cytotoxicity [Walker et al., 2000; Khalil et al., 2001; Ma

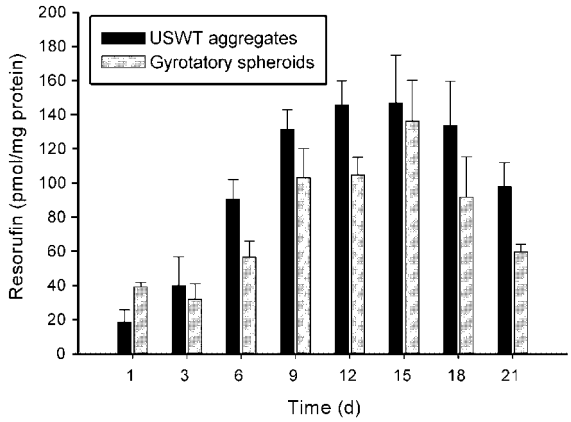

Fig. 6. Comparison of P450-1A1 activity of HepG2 USWT aggregates and gyrotatory spheroids. The aggregate cultures were pretreated at different time points by β-naphthoflavone for 24 h and then applied in EROD assays. Results are from three independent experiments with triplicate samples throughout.

et al., 2003; Xu et al., 2003a,b; Elkayam et al., 2006]. However, traditional methods producing mature multicellular aggregates generally take several days [Ma et al., 2003; Hasebe et al., 2005; Elkayam et al., 2006]. Here we report that the developed USWT produces 3D HepG2 aggregates within 30 min and that they can survive on P-HEMA surfaces with recovered cell functions during the maintenance period.

Increased junctional F-actin has been associated with cell–cell adhesion in mouse sarcoma cells and human keratinocytes. Following the initiation of cell–cell adhesion, F-actin is rapidly recruited to points of contact in order to stabilise and strengthen intercellular adhesive interactions [Chu et al., 2004; Zhang et al., 2005]. It is hypothesized that cell–cell adhesion leading to the formation of a stable 3D aggregate is enhanced by the recruitment of F-actin to regions of contact [Tzanakakis et al., 2001; Wang et al., 2006]. This response forms an ideal biomarker to identify when intercellular adhesive biomechanical interactions occur following the initiation of cell–cell contact, thus indicating the development of aggregate stability following formation. In this study, we observed an increase in junctional F-actin at points of contact between HepG2 cells in the multicellular aggregates formed in the USWT after 30 min, indicating a biological response resulting from the initiation of cell–cell contact and interaction upon exposure to the ultrasound standing wave.

We initially attempted to maintain the HepG2 USWT aggregates by the traditional gyrotatory-mediated method. However, the shaking force destroyed the USWT aggregates. P-HEMA is a matrix made of synthetic polymers that can reduce or eliminate cell adhesion to growth surfaces when applied at various concentrations [Folkman and Moscona, 1978]. Here, we showed that the HepG2 USWT aggregates can be maintained in suspensions in 2.5% P-HEMA precoated plates. The shape of USWT aggregates and internal cell–cell contacts using the junctional F-actin as a parameter remained stable during aggregate maintenance. In contrast, only small cell masses using the gyrotatory method were observed during the initial 1–3 days (Fig. 3).

In the present study, cell proliferation in two types of HepG2 3D cultures was examined by a colorimetric assay based on the cleavage of WST-1, which has been recently used in spheroid studies [Casey et al., 2001; Burleson et al., 2006; King et al., 2006; Kuijlen et al., 2006]. We showed that HepG2 cells in USWT aggregates grew in the first 3 days after formation followed by constant cell number during maintenance, while the cell number in gyrotatory spheroids remained stable over time. In addition, total cellular protein amount of USWT aggregates increased by 3 days of culture and retained constant thereafter. The cell protein amount in gyrotatory spheroids kept similar level during culture (data not shown). The kinetics of total cellular protein amount of these 3D cultures is in line with, thus supports, the proliferation results shown here.

Cellular conversion of cell-impermeable WST-1 to formazan primarily occurs at the cell surface [Berridge et al., 1996]. Reasonably, the water-soluble tetrazolium salt diffuses inside 3D cell culture like nutrients and cleaved formazan penetrates outside culture into the surrounding environment like secreted substance and cell waste [Jiang et al., 2005]. Relevant reports showed that in situ nutriment consumption rate in multicellular spheroids was equal to monolayer cells when spheroid diameter did not exceed 150 μm and nutrient consumption rate had a slight decrease (<10%) when spheroid diameter reached 250 μm, while this rate significantly decreased when spheroid size increased to over 500–1000 μm in diameter [Freyer and Sutherland, 1985; Jiang et al., 2005]. In this study, diameter of a gyrotatory spheroid was 50–70, 150–200 and 200–250 μm after 3, 9 and 18 days, respectively (Fig. 3). The

spheroid size after 21 days had no significant change compared to 18 days. USWT produced disc-like aggregates, which remained disc shape during maintenance (Figs. 2 and 3). Confocal microscopy revealed that HepG2 USWT aggregate was 5–9 cell deep (Kuznetsova et al., unpublished data), suggesting that they were approximately 40–70 μm in thickness. Furthermore, both 3D cultures retained stable during whole period of culture time under our consideration (up to 21 days). There was no significant degradation of spheroids/aggregates observed, suggesting normal exchange of nutrients and waste between cells in 3D cultures and surroundings. It is suggested that most WST-1, if not all, and its reaction product penetrate through these two types of HepG2 3D culture with limited size/thickness used in the present study.

Previous reports suggested diverse patterns in cell proliferation and cell cycle control in 3D culture systems. Human hepatocyte aggregates formed in alginate beads showed significant proliferation during 20 days of culture [Khalil et al., 2001]. However, rat hepatocyte aggregates formed on a titanium dioxide gel surface showed slightly decreased cell number over time [Nakazawa et al., 2006]. The 3D constructs produced from a C3A human hepatocyte cell line maintained a constant cell number during culture in alginate scaffolds [Elkayam et al., 2006]. In addition, human ovarian cancer multicellular aggregates cultured on an agarose gel showed a p27-associated cell cycle regulation with an increase in G0–G1 phase cell population and a decrease in S and G2-M phase cells [Xing et al., 2005]. Results from the present study demonstrate that HepG2 cells in the aggregates generated from USWT and maintained in culture on a P-HEMA-coated surface proliferated during the first 3 days and survived with cell number unchanged thereafter. HepG2 spheroids generated by the gyrotatory-mediated method had a relatively stable cell number over time. Our present data support the concept that cells in 3D cultures undergo growth arrest and cell survival which are regulated by an array of signalling pathways involved in 3D cell–cell communications, which differ from those in 2D monolayer cultures [Bates et al., 2000]. It seems that regulation of cell cycle control in 3D cultures depends on cell types and approaches used to generate the culture models. In addition, the signalling mechanisms involved in cell behavior of 3D cultures need to be fully elucidated.

It was demonstrated that rat liver spheroids prepared by the gyrotatory-mediated method showed recovered biochemical and functional characterizations including nitric oxide synthesis, albumin synthesis, enzyme activities and energy metabolism [Ma et al., 2003; Xu et al., 2003b]. HepG2 spheroids have been used as an in vitro model in hepatotoxicity studies [Xu et al., 2003a]. In addition, HepG2 aggregates cultured on alginate beads retained elevated production of various proteins related to liver functions compared to monolayer cells at similar cell density [Khalil et al., 2001]. Albumin secretion and cytochrome P450-1A1 activity are two of the most important liver-specific functional markers and both have been widely used to evaluate functionality of liver in vitro models [Juillerat et al., 1997; Peters et al., 2004; Hasebe et al., 2005]. Here, we showed that the albumin release and P450-1A1 activity from HepG2 USWT aggregates recovered after 3–6 days of aggregate formation and remained relatively consistent for at least 9 days in culture. Compared to USWT aggregates, albumin secretion and P450-1A1 activity in gyrotatory spheroids recovered later in culture, possibly due to the small number of cells fusing to aggregates during the initial days. In addition, both overall albumin secretion and P450-1A1 activity in HepG2 USWT aggregates during culture showed higher levels than gyrotatory spheroids. Our preliminary study showed increased P450-1A1 mRNA expression in HepG2 gyrotatory spheroids aged 6 days after drug induction in comparison with conventional monolayer culture (Liu et al., unpublished data). The potentially enhanced biosynthetic characteristics, such as production of P450 isozymes, proangiogenic cytokines, growth factor receptors and erythropoietin, of USWT-derived cell aggregates from HepG2 or other cell types compared to traditional cultures and the molecular basis need to be further investigated in the future.

In conclusion, the developed USWT rapidly produces 3D HepG2 multicellular aggregates, which can be maintained on P-HEMA-coated surfaces for long periods of time. HepG2 cells in the USWT aggregates show proliferating potential in the initial three days followed by constant cell number during maintenance. The liver-specific functions including albumin secretion

and cytochrome P450-1A1 activity in HepG2 USWT aggregates recover and remain relatively stable during culture. Our data also demonstrate that the functional characterization of HepG2 USWT aggregates is comparable to HepG2 spheroid cultures produced by the traditional gyrotatory-mediated method. The application of USWT to generate 3D aggregates using other cell types is currently under our studies. Recently, 3D human erythrocyte aggregates have been successfully formed in the USWT (Kuznetsova et al., unpublished data). It would be also interesting to explore the possibility of using this technique to rapidly produce co-culture of cells from different origin to investigate the interaction between different cells or tissues. Reasonably, the novel ultrasound-derived 3D culture model would not only contribute to the research of cell behavior in the very early stage of cell aggregation, but also form a part of the overall in vitro models for cell functional and toxicological studies.

ACKNOWLEDGMENTS

This work was supported by grant no. BB/C515220/1 from the Biotechnology and Biological Sciences Research Council (Swindon, UK).

REFERENCES

Bates RC, Edwards NS, Yates JD. 2000. Spheroids and cell survival. Crit Rev Oncol Hematol 36:61–74.

Bazou D, Foster GA, Ralphs JR, Coakley WT. 2005. Molecular adhesion development in a neural cell monolayer forming in an ultrasound trap. Mol Membr Biol 22:229–240.

Bazou D, Dowthwaite GP, Khan IM, Archer CW, Ralphs JR, Coakley WT. 2006. Gap junctional intercellular communication and cytoskeletal organization in chondrocytes in suspension in an ultrasound trap. Mol Membr Biol 23:195–205.

Bell E, Ivarsson B, Merrill C. 1979. Production of a tissue-like structure by contraction of collagen lattices by human fibroblasts of different proliferative potential in vitro. Proc Natl Acad Sci USA 76:1274–1278.

Berridge MV, Tan AS, McCoy KD, Wang R. 1996. The biochemical and cellular basis of cell proliferation assays that use tetrazolium salts. Biochemica 4:15–20.

Burleson KM, Boente MP, Pambuccian SE, Skubitz AP. 2006. Disaggregation and invasion of ovarian carcinoma ascites spheroids. J Transl Med 4:6.

Casey RC, Burleson KM, Skubitz KM, Pambuccian SE, Oegema TR Jr, Ruff LE, Skubitz AP. 2001. Beta 1-integrins regulate the formation and adhesion of ovarian carcinoma multicellular spheroids. Am J Pathol 159: 2071–2080.

Chu YS, Thomas WA, Eder O, Pincet F, Perez E, Thiery JP, Dufour S. 2004. Force measurements in E-cadherin-mediated cell doublets reveal rapid adhesion strengthened by actin cytoskeleton remodeling through Rac and Cdc42. J Cell Biol 167:1183–1194.

Chua KN, Lim WS, Zhang P, Lu H, Wen J, Ramakrishna S, Leong KW, Mao HQ. 2005. Stable immobilization of rat hepatocyte spheroids on galactosylated nanofiber scaffold. Biomaterials 26:2537–2547.

Elkayam T, Amitay-Shaprut S, Dvir-Ginzberg M, Harel T, Cohen S. 2006. Enhancing the drug metabolism activities of C3A – a human hepatocyte cell line – by tissue engineering within alginate scaffolds. Tissue Eng 12:1357–1368.

Folkman J, Moscona A. 1978. Role of cell shape in growth control. Nature 273:345–349.

Freyer JP, Sutherland RM. 1985. A reduction in the in situ rates of oxygen and glucose consumption of cells in EMT6/Ro spheroids during growth. J Cell Physiol 124:516–524.

Gor'kov LP. 1962. On the forces acting on a small particle in acoustical field in an ideal fluid. Sov Phys Dokl 6:773–775.

Hasebe Y, Okumura N, Koh T, Kazama H, Watanabe G, Seki T, Ariga T. 2005. Formation of rat hepatocyte spheroids on agarose. Hepatol Res 32:89–95.

Hawkes JJ, Coakley WT. 1996. A continuous flow ultrasonic cell-filtering method. Enzyme Microb Technol 19: 57–62.

Holtfreter J. 1944. A Study of the mechanisms of gastrulation. J Exp Zool 95:171–212.

Jiang Y, Pjesivac-Grbovic J, Cantrell C, Freyer JP. 2005. A multiscale model for avascular tumor growth. Biophys J 89:3884–3894.

Juillerat M, Marceau N, Coeytaux S, Sierra F, Kolodziejczyk E, Guigoz Y. 1997. Expression of organ-specific structures and functions in long-term cultures of aggregates from adult rat liver cells. Toxicol In Vitro 11:57–69.

Khalil M, Shariat-Panahi A, Tootle R, Ryder T, McCloskey P, Roberts E, Hodgson H, Selden C. 2001. Human hepatocyte cell lines proliferating as cohesive spheroid colonies in alginate markedly upregulate both synthetic and detoxificatory liver function. J Hepatol 34:68–77.

King AJ, Patrick DR, Batorsky RS, Ho ML, Do HT, Zhang SY, Kumar R, Rusnak DW, Takle AK, Wilson DM, Hugger E, Wang L, Karreth F, Lougheed JC, Lee J, Chau D, Stout TJ, May EW, Rominger CM, Schaber MD, Luo L, Lakdawala AS, Adams JL, Contractor RG, Smalley KS, Herlyn M, Morrissey MM, Tuveson DA, Huang PS. 2006. Demonstration of a genetic therapeutic index for tumors expressing oncogenic BRAF by the kinase inhibitor SB-590885. Cancer Res 66:11100–11105.

Klotz AV, Stegeman JJ, Walsh C. 1984. An alternative 7-ethoxyresorufin *O*-deethylase activity assay: A continuous visible spectrophotometric method for measurement of cytochrome P-450 monooxygenase activity. Anal Biochem 140:138–145.

Kuijlen JM, de Haan BJ, Helfrich W, de Boer JF, Samplonius D, Mooij JJ, de Vos P. 2006. The efficacy of alginate encapsulated CHO-K1 single chain-TRAIL producer cells in the treatment of brain tumors. J Neurooncol 78:31–39.

Kunz-Schughart LA, Freyer JP, Hofstaedter F, Ebner R. 2004. The use of 3-D cultures for high-throughput screening: The multicellular spheroid model. J Biomol Screen 9:273–285.

Kuznetsova LA, Coakley WT. 2004. Microparticle concentration in short path length ultrasonic resonators: Roles

of radiation pressure and acoustic streaming. J Acoust Soc Am 116:1956–1966.

Lin RZ, Chou LF, Chien CC, Chang HY. 2006. Dynamic analysis of hepatoma spheroid formation: Roles of E-cadherin and beta1-integrin. Cell Tissue Res 324:411–422.

Ma M, Xu J, Purcell WM. 2003. Biochemical and functional changes of rat liver spheroids during spheroid formation and maintenance in culture. I. Morphological maturation and kinetic changes of energy metabolism, albumin synthesis, and activities of some enzymes. J Cell Biochem 90:1166–1175.

Mellor HR, Ferguson DJ, Callaghan R. 2005. A model of quiescent tumour microregions for evaluating multicellular resistance to chemotherapeutic drugs. Br J Cancer 93:302–309.

Mueller-Klieser W. 1997. Three-dimensional cell cultures: From molecular mechanisms to clinical applications. Am J Physiol 273:C1109–1123.

Nakazawa K, Lee SW, Fukuda J, Yang DH, Kunitake T. 2006. Hepatocyte spheroid formation on a titanium dioxide gel surface and hepatocyte long-term culture. J Mater Sci Mater Med 17:359–364.

Nitori N, Ino Y, Nakanishi Y, Yamada T, Honda K, Yanagihara K, Kosuge T, Kanai Y, Kitajima M, Hirohashi S. 2005. Prognostic significance of tissue factor in pancreatic ductal adenocarcinoma. Clin Cancer Res 11: 2531–2539.

Papas KK, Constantinidis I, Sambanis A. 1993. Cultivation of recombinant, insulin-secreting AtT-20 cells as free and entrapped spheroids. Cytotechnology 13:1–12.

Peters AK, van Londen K, Bergman A, Bohonowych J, Denison MS, van den Berg M, Sanderson JT. 2004. Effects of polybrominated diphenyl ethers on basal and TCDD-induced ethoxyresorufin activity and cytochrome P450-1A1 expression in MCF-7, HepG2, and H4IIE cells. Toxicol Sci 82:488–496.

Sakai Y, Naruse K, Nagashima I, Muto T, Suzuki M. 1996. Large-scale preparation and function of porcine hepatocyte spheroids. Int J Artif Organs 19:294–301.

Santini MT, Rainaldi G. 1999. Three-dimensional spheroid model in tumor biology. Pathobiology 67:148–157.

Sutherland RM, McCredie JA, Inch WR. 1971. Growth of multicell spheroids in tissue culture as a model of nodular carcinomas. J Natl Cancer Inst 46:113–120.

Tzanakakis ES, Hansen LK, Hu WS. 2001. The role of actin filaments and microtubules in hepatocyte spheroid self-assembly. Cell Motil Cytoskeleton 48:175–189.

Walker TM, Rhodes PC, Westmoreland C. 2000. The differential cytotoxicity of methotrexate in rat hepatocyte monolayer and spheroid cultures. Toxicol In Vitro 14: 475–485.

Wang Q, Li S, Xie Y, Yu W, Xiong Y, Ma X, Yuan Q. 2006. Cytoskeletal reorganization and repolarization of hepatocarcinoma cells in APA microcapsule to mimic native tumor characteristics. Hepatol Res 35:96–103.

Xing H, Wang S, Hu K, Tao W, Li J, Gao Q, Yang X, Weng D, Lu Y, Ma D. 2005. Effect of the cyclin-dependent kinases inhibitor p27 on resistance of ovarian cancer multicellular spheroids to anticancer chemotherapy. J Cancer Res Clin Oncol 131:511–519.

Xu J, Ma M, Purcell WM. 2003a. Characterisation of some cytotoxic endpoints using rat liver and HepG2 spheroids as in vitro models and their application in hepatotoxicity studies. I. Glucose metabolism and enzyme release as cytotoxic markers. Toxicol Appl Pharmacol 189:100–111.

Xu J, Ma M, Purcell WM. 2003b. Biochemical and functional changes of rat liver spheroids during spheroid formation and maintenance in culture. II. Nitric oxide synthesis and related changes. J Cell Biochem 90:1176–1185.

Yuhas JM, Li AP, Martinez AO, Ladman AJ. 1977. A simplified method for production and growth of multicellular tumor spheroids. Cancer Res 37:3639–3643.

Zhang J, Betson M, Erasmus J, Zeikos K, Bailly M, Cramer LP, Braga VM. 2005. Actin at cell-cell junctions is composed of two dynamic and functional populations. J Cell Sci 118:5549–5562.